

# Energetics and bonding properties of the Ni/ $\beta$ -SiC (001) interface: an *ab-initio* study

G. Profeta, A. Continenza

*Istituto Nazionale di Fisica della Materia (INFM)*

*Dip. Fisica, Univ. degli Studi dell'Aquila, 67010 Coppito (L'Aquila), Italy*

A. J. Freeman

*Department of Physics and Astronomy*

*Northwestern University, Evanston, IL 60208 (U.S.A.)*

## Abstract

We investigate the adsorption of a Ni monolayer on the  $\beta$ -SiC(001) surface by means of highly precise first-principles all-electron FLAPW calculations. Total energy calculations for the Si- and C-terminated surfaces reveal high Ni-SiC adsorption energies, with respect to other metals, confirming the strong reactivity and the stability of the transition metal/SiC interface. These high binding energies, about 7.3-7.4 eV, are shown to be related to strong *p-d* hybridization, common to both surface terminations and different adsorption sites and despite the large mismatch, can stabilize overlayer growth. A detailed analysis of the bonding mechanism, hybridization of the surface states, charge transfer and surface core level shifts reveals the strong covalent character of the bonding. After a proper accounting of the Madelung term, the core level shift is shown to follow the charge transfer trend.

PACS numbers: 73.20.-r, 73.20.At, 82.65+r, 73.20.Hb, 68.55.-a

## I. INTRODUCTION

The promising mechanical and electronic properties of silicon carbide are stimulating many studies focused on the application of its semiconducting and extreme structural properties. In fact, the interest towards SiC is twofold: on one hand SiC is a high-strength composite and high-temperature ceramic seal<sup>1</sup> and is considered a basic material for detectors and devices operating in high radiation environments, in space applications, in medicine and industry. In this regard, as pointed out in recent papers<sup>2,3</sup>, fundamental interest is focused on the investigation of the nature of bonding and the origin of adhesion at metal-ceramic interfaces: the bonding properties, are in fact strongly dependent on the metal and on the ceramic and may lead to nonreactive systems<sup>4</sup> (e.g. MgO/Ag) as well as to reactive systems (e.g. SiC/Al). On the other hand, SiC represents an interesting semiconductor. It has a wide band gap (2.2 eV); carrier mobilities and drift velocities exceed the corresponding values in Si by more than a factor of two. Together with its thermal stability, these characteristics allow for high-power and high-frequency operation at elevated temperatures<sup>5</sup>. However, application of SiC-based semiconducting devices requires a deep understanding of metal contact formation.

As in the case of other semiconducting materials, knowledge of the reactivity and of the detailed electronic structure of the metal-semiconductor interface is the first step towards device design and performance control. An excellent review by Kaplan and Bermudez<sup>6</sup> presents results of metal deposition on various SiC surfaces obtained by different experimental techniques. Among the metals studied, Ni seems to have the highest stable temperature contacts, an essential requirement to exploit the properties of SiC: Ni overlayers were reported to be thermally stable up to 800° C; at higher temperatures the silicide formation process starts leading to a silicide-SiC contact. During heat treatment, the formation of silicides with different stoichiometry was also reported. The silicidation process, that is metal deposition followed by rapid thermal annealing (RTA), is very common in silicon-based technology and many experimental and theoretical works were devoted to understanding this process and, in particular, to characterize the multiple silicide phases and their interface with Si. We cite, specifically, the recent and extended work by the Vienna group<sup>7</sup>, which studied the cohesive, electronic and structural properties of various TM-silicides (TM=Fe, Ni, Co), including different bulk phases, surfaces and interfaces with Si. Looking at the epitaxially stabilized structures of Fe, Co, and Ni silicides they also discovered new artificial materials with interesting elastic properties that they called *supersoft*. As an example, FeSi<sub>2</sub> in the C1 (fluorite) structure, as well as CoSi and NiSi in the B2 (sodium chloride) structure, show zero strain energy under biaxial strain on a (100) substrate. However, these phases are not stable phases and the lattice mismatch with the Si(100) surface is too large to encourage epitaxial growth.

As is well-known, pseudomorphic epitaxial growth of ultrathin metal films on a substrate results in a strain on the film due to the mismatch between the lattice constant of the film and the substrate. Especially interesting is the stabilization of metastable phases that can be achieved using suitable substrates, offering strong adhesion energy and close matching conditions. Within this framework, the investigation of the Ni-SiC(001) interface becomes particularly relevant in view of the study of a possible Ni-silicide/SiC(100) system. Moreover, from an experimental point of view, the study of this interface is far from the deep

understanding achieved for the silicide-silicon interfaces, and in fact the real structure of the interface is still unknown. Finally Ni/SiC interface, deserves attention in its own right, since this rather simple system can provide important information on the nature of the transition-metal SiC bond. For all these reasons, we present here the first *ab-initio* analysis of the Ni/SiC interface at the first stage of deposition, focusing on the system formed by a Ni monolayer adsorbed on a SiC(001) substrate.

The paper is organized as follows: in Sect. II we give details of the calculation, then we discuss results for the structural (Sect. III) and electronic properties (Sect. IV) for all the different geometries considered; and finally, in Sect. V, we discuss the surface core-level shifts and draw conclusions (Sect. VI).

## II. TECHNICAL DETAILS

The calculations are performed using the all-electron full-potential linearized augmented plane wave (FLAPW) method<sup>8</sup> within density functional theory in the local density approximation (LDA)<sup>9</sup> according to the Hedin-Lundqvist parametrization of the exchange-correlation energy. The surface is modelled in a superslab geometry with a slab that includes seven (six) silicon layers and six (seven) carbon layers to simulate the substrate in the case of the silicon (carbon) terminated surface with a Ni adsorbate on both surfaces and 10.5 Å (equivalent to about ten SiC bilayers) for the vacuum region. The calculated bulk SiC equilibrium lattice constant  $a_{SiC} = 4.35$  Å agrees (within 0.2 %) with the experimental value. The muffin-tin radii used are  $r_{mt}^{Si} = 1.8$  a.u.,  $r_{mt}^C = 1.5$  a.u. and  $r_{mt}^{Ni} = 2.0$  a.u.. The Ni 3*d* and 4*s*, Si 3*s* and 3*p*, C 2*s* and 2*p* were treated as valence electrons. We used a plane wave cutoff  $k_{max} = 3.8$  a.u. for the basis set, 8 a.u. for the potential and charge density representation and a  $6 \times 6 \times 4$  Monkhorst-Pack<sup>10</sup> *k*-point mesh for integration over the Brillouin zone; 64 *k* points in the irreducible wedge of the Brillouin zone were used to calculate the density of states. Our present implementation includes total energy and atomic force calculations, which allows full structure optimization using a *quasi*-Newton<sup>11</sup> scheme. The stable configuration is found when the 3*n*-dimensional force vector of the system with *n* atoms is approximately zero (i.e. forces on each atom smaller than 1.0 mHtr/a.u.). For all the structures considered, we used the same supercell to achieve consistency for the total energy. Convergence, within 1 mHtr in the total energy was checked as a function of *k*-points integration,  $k_{max}$  value and number of layers used in the calculation.

## III. STRUCTURAL PROPERTIES OF A NI MONOLAYER ON SiC(100)

A top view of the unit cell adopted for the simulation is illustrated in Fig.1. The most stable reconstruction for the clean Si-terminated (Si-SiC)(001) surface is calculated to be  $p(2 \times 1)$  with unbuckled Si dimers<sup>12</sup> which has a total energy only a few meV/atom lower than the ideal  $p(1 \times 1)$ . For the C-terminated (C-SiC)(001) surface, the most likely stable reconstructions are  $c(2 \times 2)$  and  $p(2 \times 1)$ <sup>13</sup>.

With only few exceptions, materials with low surface energy tend to grow on high-surface-energy materials, while the reverse is usually inhibited. Ni has a high surface energy, about 0.96 eV/atom, a value much higher than in non-transition metals and about 2/3 of the upper

limit for transition metals (Re, Os)<sup>16</sup>. In a crude approximation, neglecting the interaction energy between substrate and overlayer, Ni growth should not be favored when compared to other low surface-energy metals. As anticipated in the Introduction, however, transition metals with partially occupied *d* shells show large interaction energy with reactive ceramics that may stabilize overlayer growth. We demonstrate here that this is the case for the Ni/SiC interface.

For this particular interface no information, to our knowledge, is available regarding favored adsorption sites and possible surface reconstructions: deposition of Ni on SiC(001) leads to Ni-Si intermixing at sufficiently high temperature and no experimental studies are available on the non-intermixed Ni-SiC phase. Due to the lack of experimental information, our calculations on the Ni-SiC(001) interface assume a (1×1) in-plane periodicity. This system allows the study of the bonding properties of the transition metal (TM) on both the Si-terminated and C-terminated SiC surface and gives insights into possible geometries and more complicated reconstructions. In the ideal (1×1) reconstruction, in fact, there are four possible adsorption sites (Fig 1): antibridge, bridge, four-fold (hollow) and on-top sites that constitute total energy extrema, due to the surface symmetries. From a geometrical point of view, the four adsorption sites are rather different and hence different bonding properties of the TM atom can be expected. For each site, we calculated the equilibrium structure and the adsorption energy, i.e. the energy gained in the adsorption process, which we define as:

$$E_{ads} = -\frac{1}{2}(E_{s+ad} - E_s - 2E_{ad})$$

here,  $E_{s+ad}$  is the total energy of the SiC-Ni system,  $E_s$  is the total energy of the clean surface and  $E_{ad}$  that of the free Ni atom. Results for the Si and C-terminated surfaces are reported in Table I (we do not report values for the on-top site since it shows very low adsorption energy and is therefore not favored).

As far as the substrate is concerned, all the geometries considered lead to a small relaxation of the upper SiC layer (only in the hollow-site case does the outward relaxation of the Si and C layer reach about 0.1 Å). The height of the adatom on the substrate increases in going from the hollow site (the most open structure) to the antibridge (the most closed), in both terminations. In particular, in the hollow site Ni is very close to the surface plane, about 1 Å in the Si-terminated and 0.5 Å for the C-terminated case. The four-fold adsorption site was first proposed<sup>17</sup> for Co/Si(001); in this case the adatom height with respect to the substrate was inferred to be  $\simeq 0$ , implying that Co would lie in the topmost silicon plane restoring the (1×1) reconstruction. This picture is consistent with the results we find: the larger in-plane lattice constant of Si(001), with respect to SiC, could favour penetration of the adatom into the surface, leading to an adatom height lower than in the SiC case.

The difference observed between the Si and C terminations is a consequence of the smaller atomic radius of C with respect to Si, while the adsorption energies are similar (within  $\simeq 0.3$  eV) in all the systems investigated (see Table I). This result is interesting since the adsorption sites considered and the two terminations are quite different. In the hollow site, the Ni atom is four-fold coordinated with silicon (carbon), while in the bridge site the coordination is only two-fold. On the other hand, the antibridge site, which is also two-fold coordinated, has to form bonds with the dangling-bonds from the two top-most surface atoms which point towards the bridge site. This reduces the adsorption energy and makes the antibridge unstable compared to the bridge site. We should remark, however, that

substrate relaxation plays an important role: in fact, if we keep the substrate unrelaxed, we find that the configuration with the adatom in the bridge site at its equilibrium position has higher energy (about 1 eV) with respect to the completely relaxed structure for the hollow site.

As a general remark, we point out that the adsorption energies calculated for the three sites considered are all larger with respect to those calculated in the case of an Al adatom in the same configurations<sup>18</sup>. The computed values for the adsorption energy are referred to a clean, unreconstructed but relaxed SiC surface and a free Ni atom. In order to estimate the binding energy of a Ni monolayer on the SiC surface, we calculated the total energy of an unsupported Ni monolayer at the SiC lattice constant. The total energy difference per atom between a free Ni atom and a Ni free-standing monolayer in a square lattice is 1.5 eV/atom, showing that in the choosen configuration the Ni-Ni bond-energy is smaller than the Ni-Si, Ni-C. The high adsorption energies found indicate that Ni/SiC(001) belongs to the chemisorption class ( $E_{ads} > 0.5$  eV) instead of the physisorption class ( $E_{ads} < 0.5$  eV), thus confirming that Ni/SiC is a reactive metal-ceramic interface where bond hybridization plays an important role. In particular, it is straightforward to identify the  $p$ - $d$  hybridization, characteristic of TM-silicides and carbides, as having major responsibility for the bonding. The same bonding features are expected to be found for Fe and Co (that also form silicides and carbides<sup>6,15</sup>), as discussed in greater detail below.

#### IV. ELECTRONIC PROPERTIES

The shape of the energy landscape of Ni on SiC appears quite flat for the Si-terminated surface, and in general the high adsorption energy of the bridge and hollow sites deserves a discussion of the electronic properties of both configurations. In the following, we discuss the electronic and bonding properties for the Ni adatom in both sites separately.

##### A. Bridge Site

In this geometry the Ni adatoms occupy the cation (anion) sites and therefore are in line with the Si (C)  $sp^3$  dangling bonds. In the clean Si-SiC surface, the surface states originate from the surface dangling bonds and lie above the bulk valence band maximum, while for the C-SiC surface in the  $(1 \times 1)$  reconstruction, the surface states appearing in the bulk band gap are contributed by dangling-bonds as well as back-bonds of the surface C atoms<sup>12</sup>. We expect that the interaction with Ni adatoms should partially remove these states. In Fig. 2 we show the projected density of states (PDOS) on different atom sites for the Si-terminated and C-terminated surface resolved according to surface symmetry, from the inner "bulk" layer (Si or C) to the Ni adatom. In the figures shown, we set the zero of the energy axis to the Fermi level that, consistent with other metal-semiconductor interfaces, lies within the semiconductor band gap even at monolayer coverage.

The two central layers (lower panel in Fig.2) of the SiC slab are quite representative of bulk SiC, showing a well defined valence band maximum and a shape which closely resembles the PDOS of bulk SiC. The interaction with the Ni adatom is localized within the topmost surface layers. Let us first discuss the Si-terminated surface. As already known from studies

on TM silicides<sup>19</sup>, bonding between TM and silicon atoms is due to hybridization of the Si-3*p* with the TM *d* states; in the present case, we also find a partial contribution from Si-*s* states, coming from rehybridization of the original *sp*<sup>3</sup> orbitals. In the same figure, we show the PDOS for the Ni *d* states resolved into atomic-like *d*-components. As a general feature, present in all the structures considered, we found a noticeable broadening of the Ni-*d* bandwidth (about 5 eV) when compared to the narrow *d*-band of the Ni monolayer ( $\sim 1$  eV).

The bonding properties are now quite clear: there is a strong hybridization between the Si *p* states (mainly with  $p_x, p_z$  character) with some of the Ni *d*-states with mainly  $d_{xz}, d_{3z^2-r^2}$  character with a spatial distribution pointing directly towards the Si atom dangling bonds: as a result, these states have a larger band-width and are pushed to higher binding energy with respect to the other *d* states that remain in a non-bonding configuration. On the surface Si layer we find the presence of a pronounced feature with  $p_x$ -character above (by  $\simeq +1\text{eV}$ ) and below (by  $\simeq -3\text{eV}$ )  $E_F$  and a broadening of the *s* band.

Evidence of the character of these states comes from the plot of the charge density (shown in Fig. 3) due to eigenfunctions whose eigenvalues belong to the two main peaks (the bonding one at about -3 eV and the antibonding one at 1 eV). While the charge density related to the bonding peak (Fig. 3(a)) is well delocalized among Ni and Si atoms (with some resonance states into the bulk), the anti-bonding peak (Fig.3(b)) shows very low charge density in-between the Si and Ni atoms with a horizontal shape characteristic of non-bonding  $p_x$  states, well localized in the surface layer.

Analogous bonding features can be found in the C-terminated surface: in this case, however, the bond involves C-*p* orbitals combinations with mainly Ni  $d_{xz}$  and  $d_{x^2-y^2}$  states showing a quite large bandwidth in the PDOS; the C-1*s* are found at higher binding energies (not shown in Fig. 2). The other *d*-orbitals (i.e.  $d_{xy}, d_{yz}, d_{3z^2-r^2}$ ) are confined to a more limited energy range around -1 eV below  $E_F$ . Correspondingly, we find that the *p*-states of the C-surface site are smeared over the same energy range of the Ni-*d* states leading to a total bandwidth of 7-8 eV. Again, we can distinguish bonding-antibonding features whose energy position is clearly symmetry dependent. In fact, we find a large splitting (5 eV) for the  $p_x$  states hybridized with Ni- $d_{xz}$  (cf. strong feature at -4 eV) that makes the antibonding combination completely empty, while the bonding-antibonding splitting is only of 3-4 eV for  $p_y$  and  $p_z$  states.

To further ascertain the difference with the Si-terminated surface, we consider the surface geometry in the two cases. While Ni sits at 1.52 Å above the Si-terminated surface, it is almost coplanar with the C-topmost layer. This draws more spectral weight into the  $p_x$  orbital which better fits the Ni  $d_{xz}$  and  $d_{x^2-y^2}$  orbitals. The bonding features observed for the  $p_z$  and  $p_y$  states are explained recalling that states at the VBM in the clean C-terminated surface are contributed by the dangling bonds but also by back-bonds of the surface C-atoms (which, due to symmetry, also involve  $p_z$  and  $p_y$  combinations). In the Si-terminated case, the larger adatom height from the surface favors an overlap between Ni- $d_{3z^2-r^2}$  and Si- $p_z$  states, leaving the  $p_y$  component almost not affected by the bond.

## B. Hollow sites

Due to the symmetry of the four-fold adsorption site and the small vertical distance from the surface atoms, the Ni states involved in the bonding have mainly in-plane  $d_{xy}$  and  $d_{x^2-y^2}$  symmetry, as is evident from Fig.4. In fact, we find a strong hybridization of  $d_{xy}$ -type states with the Si- and C-  $p$  states in the Si- and C-terminated surface, respectively; as in the bridge sites discussed previously, these states form a bonding-antibonding configuration. In the C-terminated surface, the energy splitting is more pronounced due to the larger orbital overlap: in fact, the anti-bonding  $d_{xy}$ - $p_x$  peak appears at about 1 eV above  $E_F$ . In both terminations, moving from the bulk to the surface layer, we find the appearance of a feature with  $p_z$  character at  $E_F$ , located in the middle of the SiC bulk band-gap. In order to better bring out the nature of this feature, we plot in Fig.5(a) the projected DOS on C atoms belonging to different layers. We observe that this same feature has a significant spectral weight also in the sub-surface layers (C2 and C3 in Fig.5(a)). These peculiar states originate from a vertical non-bonding combination of Ni  $d_{3z^2-r^2}$  and  $p_z$  orbitals from the atoms underneath the Ni adatom; their spatial extension and non-bonding character are shown in Fig. 5(b) where the charge density corresponding to states within 1 eV below the Fermi energy is plotted. While this peak falls right at  $E_F$  in the Si-terminated surface, it is completely filled in the C-terminated surface.

## V. SURFACE-CORE-LEVEL SHIFT

The surface-core-levels shifts are particularly relevant from an experimental point of view, since they are directly accessible by photoemission spectroscopy and can give insights on the adatom position and surface reconstruction. We calculate the surface-core-level shift as the difference of the core-level eigenvalue corresponding to the surface atom (*e.g.* Si- $2p_{3/2}$  and C-1s) and that of the central (bulk) layer. It is clear that within this method we neglect so-called final-state effects, while taking into account only initial-state effects. Now, it is a common procedure to associate the observed core-level shifts with charge transfer between the atoms, in our case Si (C) and the Ni adatom; however, the variation of the core-level eigenvalues is strictly related to changes in the total potential on the atom core, which is mainly due to two different contributions<sup>20</sup>: an intra-atomic effect, due to charge transfer, and an inter-atomic contribution, namely the Madelung potential, that acts in the opposite direction. A measure of the charge transfer can be achieved by comparing the charge in the muffin-tin (MT) region of the atom considered and the one in the inner layer taken as reference.

Figure 6 shows the results obtained for the structures analyzed. Even if the definition of charge transfer is not unique, the results show a well defined trend, namely, a charge transfer from surface Si (C) to Ni, while all the other atoms remain bulk-like. The charge transfer is rather small ( $\sim 0.1$  to  $\sim 0.2$  electrons) in all the structures considered. This is consistent with the trend observed in the core-level-shifts for all the structures except for the Si-terminated with Ni in the bridge-site. In this last case, we observe a positive shift towards lower binding energy, even if the surface atom loses charge. It is evident that a direct relationship between charge transfer and core-level shift is misleading in this case.

The correct behaviour is recovered if we subtract the Madelung potential from the core-level binding energy<sup>21</sup>. The result is shown in Fig.6 (a)(dashed line). We see that after a proper accounting of the Madelung term the core-level shift follows the charge transfer trend; we point out that subtraction of the Madelung term in the other structures does not change the overall trend. The calculated core-level shift to lower binding energy of the Si  $2p_{3/2}$  state agrees with the trends observed by photoemission spectroscopy<sup>5</sup>, but we showed that this does not directly imply a positive charge transfer towards the surface Si atom. As a general remark, we point out that the order of magnitude of the charge transfer<sup>20</sup> and of the core-level shift are consistent with the covalent character discussed previously for the bond between Ni and SiC where a strong charge transfer is not expected.

## VI. CONCLUSIONS

The highly precise FLAPW method<sup>8</sup> was used to understand the adsorption of a Ni monolayer on the  $\beta$ -SiC(001) surface. The adsorption energy on both the Si- and C- terminated surfaces is found to be quite high and differs only slightly between the different adsorption sites (bridge and hollow). We predict, therefore, that the SiC(001) surface represents a strong reactive surface for Ni and could therefore be a suitable substrate for the growth of metallic Ni and the formation of Ni-silicides. We explained the high adhesion energy in terms of a strong covalent Si- (C-)Ni bond. In all the surface geometries investigated, the Si- (C-) $p$  orbitals are strongly hybridized with the Ni- $d$  states resulting in bonding-antibonding features and a consequent partial lowering of the Ni- $d$  density of states at  $E_F$ . The surface states are well localized in the surface region (Ni overlayer and the top-most Si (C) layer) for Ni in the bridge-site, while a deeper penetration of the antibonding state of  $p_z$ - $d_{3z^2-r^2}$  character into the SiC bulk is observed for Ni in the hollow-site. We calculated the surface-core-level shifts and found them in agreement with available experimental data; we also showed that the Madelung contribution should be correctly taken into account to relate the observed core-level-shifts to the charge-transfer.

## VII. ACKNOWLEDGMENTS

Work at Northwestern University was supported by the U.S. Department of Energy (under grant No. DE-F602-88ER45372).



## REFERENCES

- <sup>1</sup> H. G. Bohn, J. M. Williams, C. J. McHargue, and G. M. Begun, J. Mater. Res. **2**, 107 (1987)
- <sup>2</sup> J. Hoekstra and M. Kohyama, Phys. Rev. B **57**, 2334 (1998)
- <sup>3</sup> M. Kohyama and J. Hoekstra, Phys. Rev. B **61**, 2672 (2000)
- <sup>4</sup> Chun Li, Ruquian Wu, A. J. Freeman and C. L. Fu, Phys. Rev. B **48**, 8317 (1993)
- <sup>5</sup> H. Höchst, D. W. Niles, G. W. Zajac, T. H. Fleisch, B. C. Johnson and J. M. Meese, J. Vac. Sci. Technol. B **6** (4), 1320 (1988)
- <sup>6</sup> R. Kaplan and V. M. Bermudez, in *Properties of Silicon Carbide -EMIS Datareviews Series, No. 13* edited by G. L. Harris (INSPEC, London, 1995) p. 101
- <sup>7</sup> E. G. Moroni, R. Podloucky and J. Hafner, Phys. Rev. Lett. **81**, 1969 (1998); R. Stadler, D. Vogtenhuber and R. Podloucky, Phys. Rev. B **60**, 17112 (1999)
- <sup>8</sup> H. J. F. Jansen and A. J. Freeman, Phys. Rev. B **30**, 561 (1984); E. Wimmer, H. Krakauer, M. Weinert and A. J. Freeman, *ibid.* **24**, 864 (1981)
- <sup>9</sup> P. Hohenberg and W. Kohn, Phys. Rev. **136**, B864 (1984); W. Kohn and L. J. Sham, *ibid.* **145**, 561 (1966)
- <sup>10</sup> H.J.Monkhorst and J.D.Pack, Phys. Rev. B **13**, 5188 (1976)
- <sup>11</sup> C. G. Broyden, J. Inst. Math. Appl. **6**, 222 (1970)
- <sup>12</sup> A. Catellani, G. Galli, F. Gygi, F. Pellacini, Phys. Rev. B **57**, 12255 (1998)
- <sup>13</sup> A Catellani, G. Galli, F. Gygi, Phys. Rev. Lett. **77**, 5090 (1996)
- <sup>14</sup> L. Wenchang, Z. Kaiming and Xie Xide, Phys. Rev. B **45**, 11048 (1992)
- <sup>15</sup> J. Häglund *et al.*, Phys. Rev. B **43**, 14400 (1991)
- <sup>16</sup> W. E. Pickett and Steven C. Erwin, Phys. Rev. B **41**, 9756 (1990)
- <sup>17</sup> H. L. Meyerheim, U. Döbler and A. Puschmann, Phys. Rev. B **44**, 5738 (1991)
- <sup>18</sup> L. Wenchang, Z. Kaiming and X. Xide, Phys. Rev. B **45**, 11048 (1992)
- <sup>19</sup> S. R. Nishitani, S. Fujii, M. Mizuno, I. Tanaka, H. Adachi, Phys. Rev B **58**, 9741 (1998)
- <sup>20</sup> S. Ossicini, C. Arcangeli and O. Bisi, Phys. Rev. B **43**, 9823 (1991)
- <sup>21</sup> M. Weinert, E. Wimmer and A. J. Freeman, Phys. Rev. B **26**, 4571 (1982)

# TABLES

TABLE I. Equilibrium bond-length ( $d_{Ni-X}$ ) between Ni and (Si, C) surface atoms, vertical distances between the Ni adatom from the surface plane ( $h$ ) (in Å) and adsorption energies (in eV)

Si-terminated	Antibridge	Bridge	Hollow
$d_{Ni-Si}$	2.18	2.16	2.38
$h$	1.55	1.52	1.00
$E_{ads}$	6.61	7.42	7.40
C-terminated			
$d_{Ni-C}$	1.82	1.78	2.22
$h$	0.97	0.92	0.50
$E_{ads}$	6.90	7.35	7.30

## FIGURES

FIG. 1. Side and top view of SiC(001) ( $1 \times 1$ ) showing the different Ni adsorption sites.

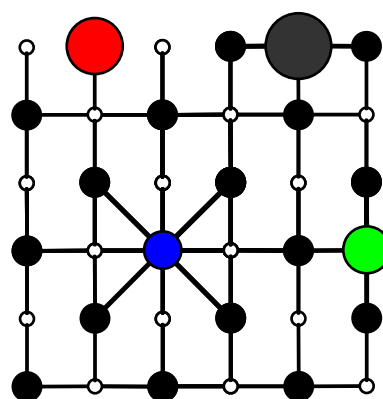
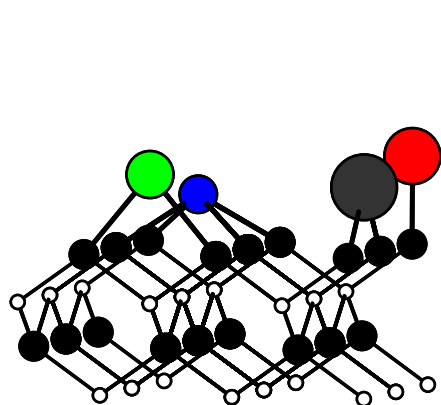
FIG. 2. PDOS for the bridge adsorption site in the (a) Si and (b) C terminated surface. Upper panel: Ni  $d$ -projected density of states; central panel: topmost surface Si (a) and C (b) layer,  $s$  (dotted line),  $p_x$  (bold line),  $p_y$  (dashed line),  $p_z$  (thin line) contributions; lower panel: bulk Si (a) and C (b) layer  $s$  (dashed line) and  $p$  (thin solid line) contributions.

FIG. 3. Charge density plot for the (a) bonding and (b) antibonding peak for the Si-terminated surface with Ni in the bridge adsorption site. The charge densities are constructed taking into account only states belonging to the peak at -3 eV (for the bonding) and at 1eV (for the antibonding state).

FIG. 4. PDOS for the hollow adsorption site. Symbols as in Fig. 2

FIG. 5. Panel (a):  $p_z$ -like contribution to the density of states from carbon atoms at different slab layers; panel (b): charge density plot due to states up to 1 eV below  $E_F$ . Both panels refer to the hollow-site geometry, labels C1 up to C4 refer to sites from surface down to bulk layers.

FIG. 6. Surface-core level shifts for Si  $2p_{3/2}$  for (a) Ni in the bridge-site and (c) Ni in the hollow-site and total charge inside the Si-MT (insets therein). Panel (b) and (d): C-1s core level shift and total MT charge (insets) for the bridge and hollow site, respectively.






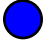


-  Ni bridge
-  Ni anti-bridge
-  Ni on-top
-  Ni hollow
-  Si
-  C

Fig. 2- Profeta et al.

(a) Si-terminated

(b) C-terminated

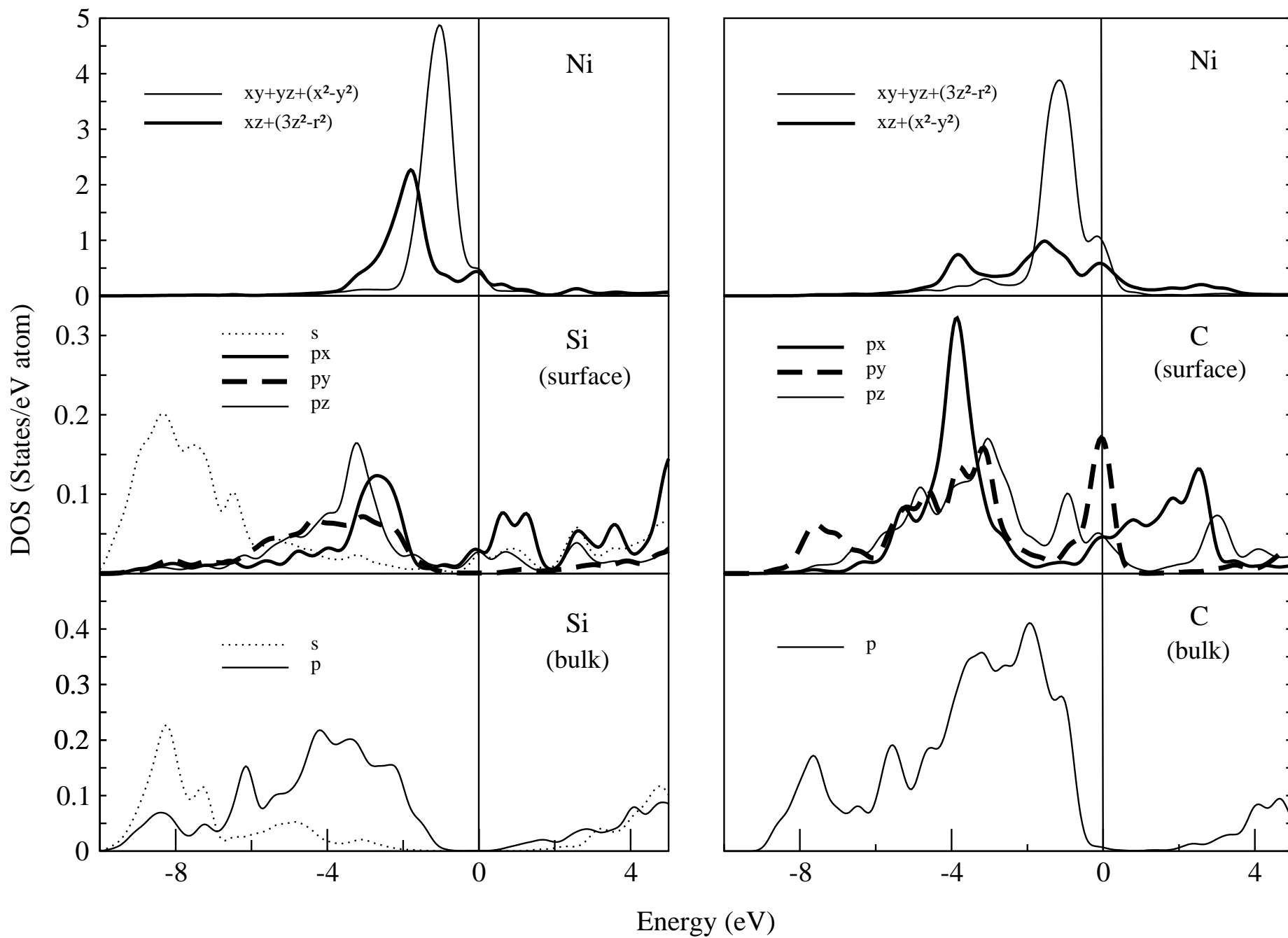


Fig. 3 - G. Profeta et al.

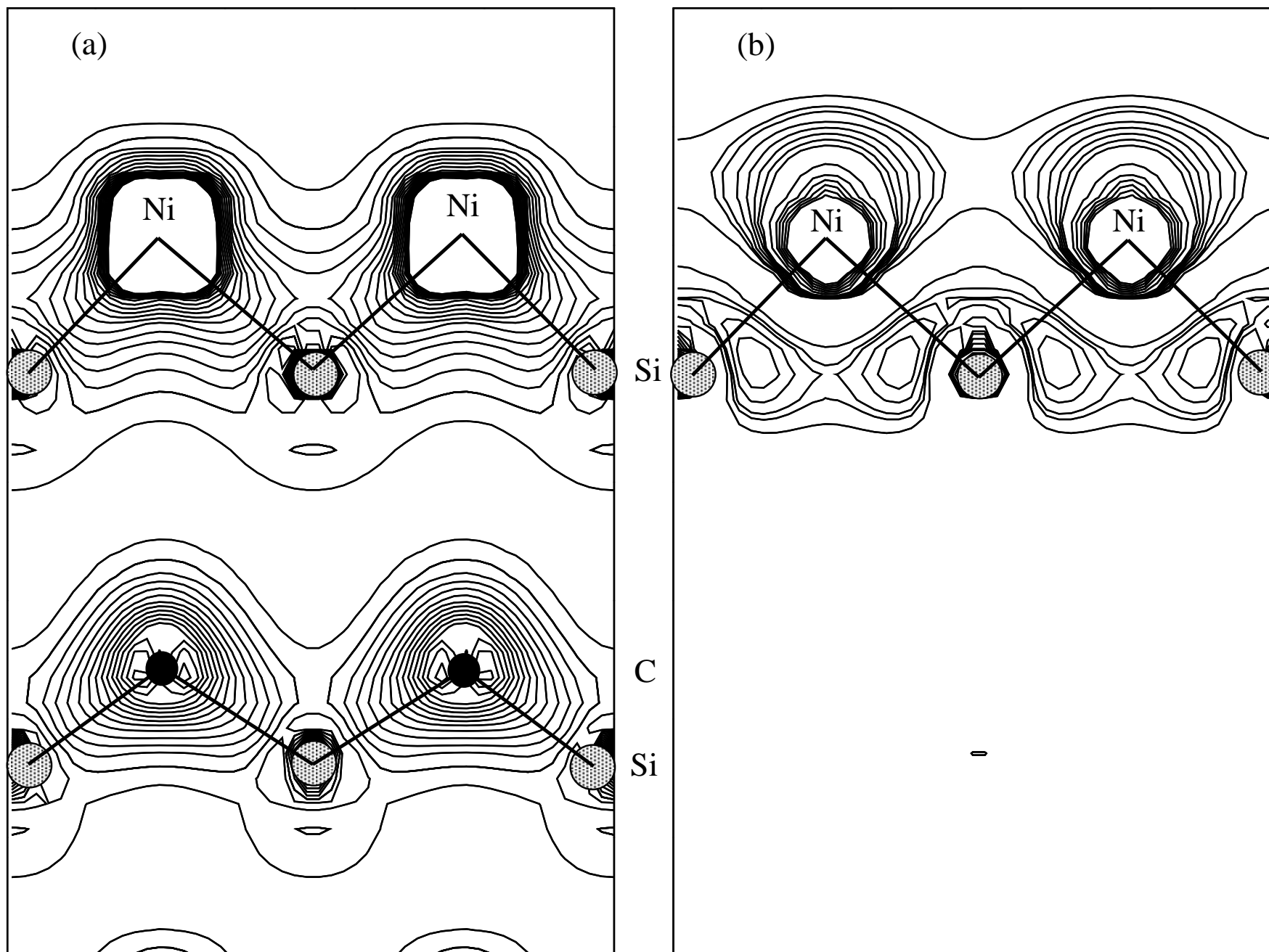
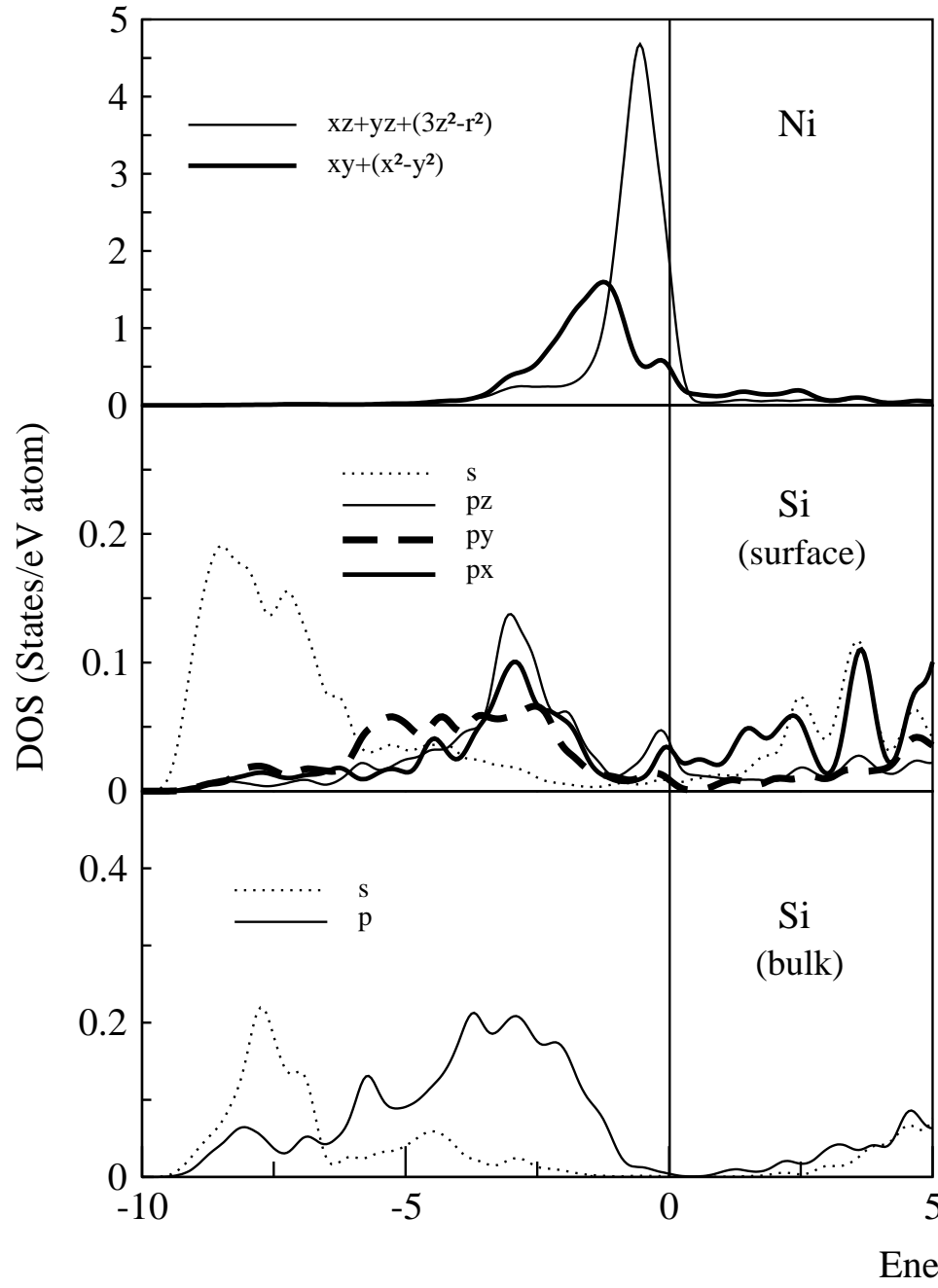
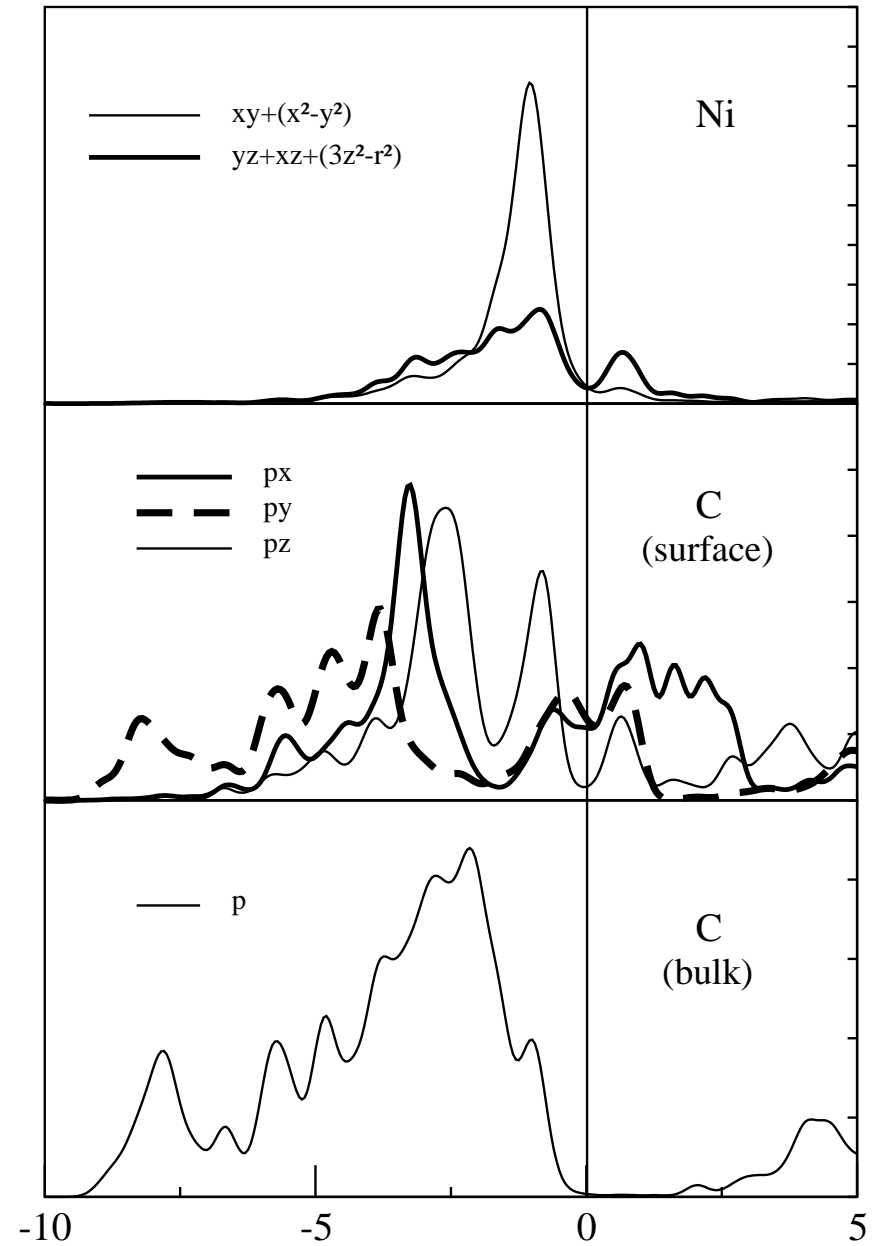


Fig. 4- Profeta et al.

(a) Si-terminated



(b) C-terminated



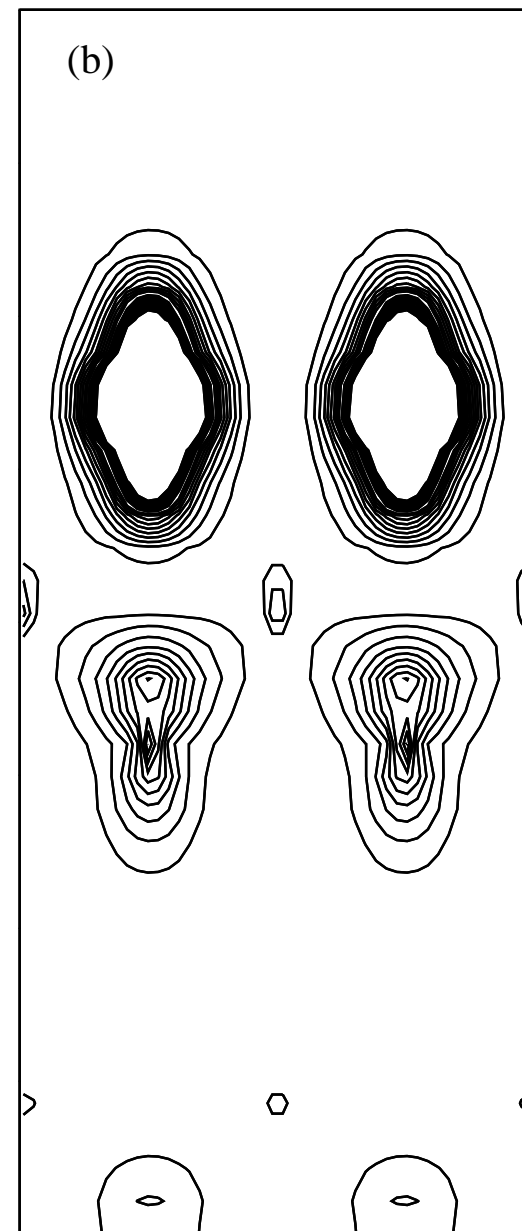
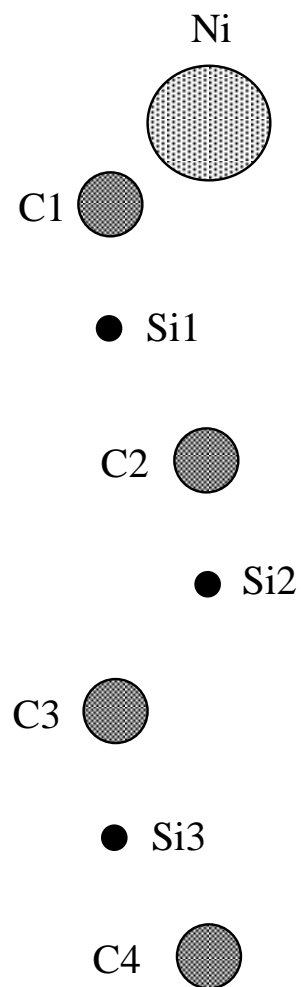
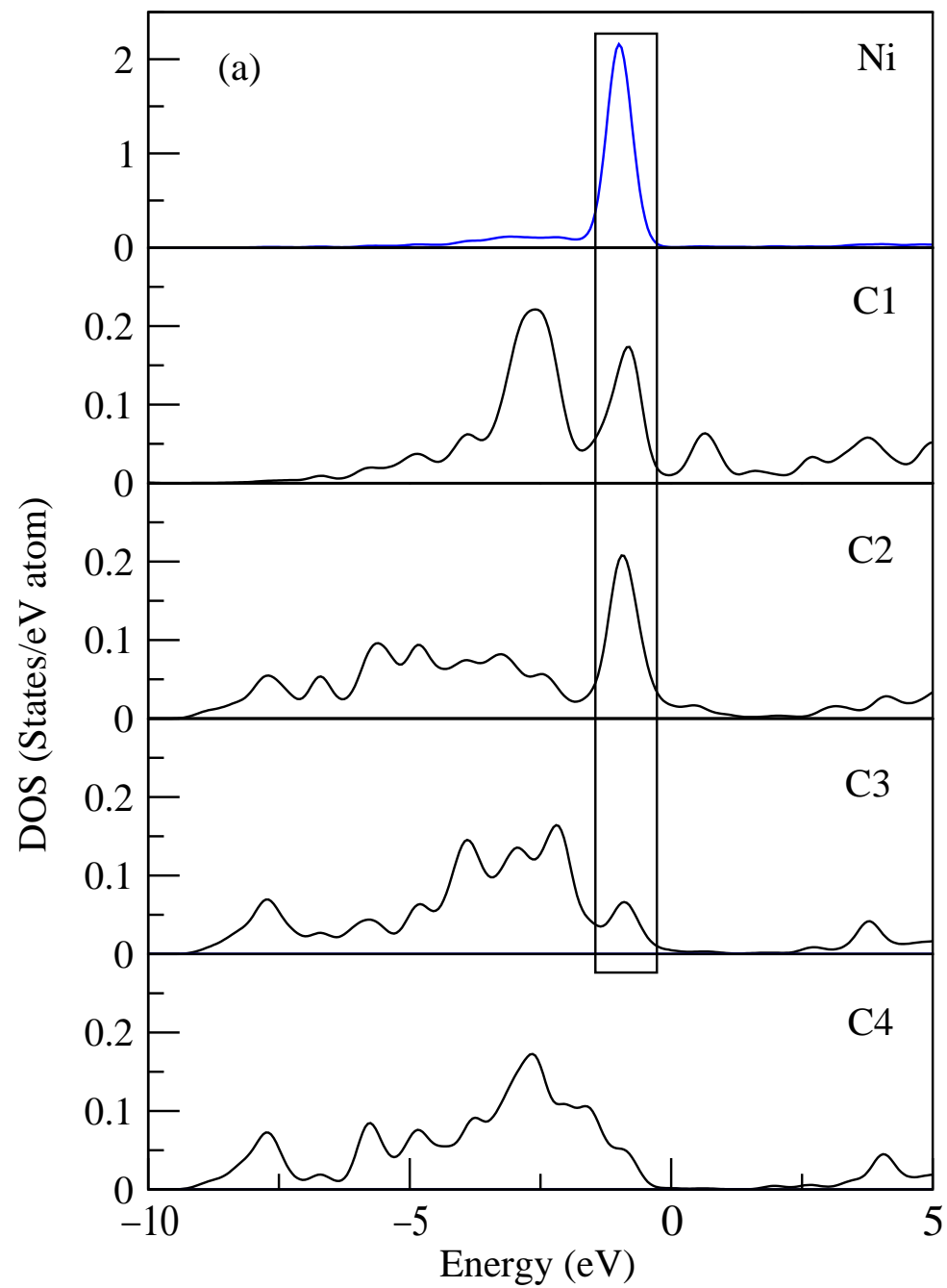


Fig. 5 – Profeta et al.



Fig. 6 - G. Profeta et al.

